Lasers Med Sci (2013) 28:815–822
DOI 10.1007/s10103-012-1166-4

ORIGINAL ARTICLE

# The efficacy of the use of IR laser phototherapy associated to biphasic ceramic graft and guided bone regeneration on surgical fractures treated with wire osteosynthesis: a comparative laser fluorescence and Raman spectral study on rabbits

**Antônio Luiz Barbosa Pinheiro · Nicole Ribeiro Silva Santos · Priscila Chagas Oliveira · Gilberth Tadeu Santos Aciole · Thais Andrade Ramos · Tayná Assunção Gonzalez · Laís Nogueira da Silva · Artur Felipe Santos Barbosa · Landulfo Silveira Jr**

Received: 4 October 2011 / Accepted: 12 July 2012 / Published online: 26 July 2012


**Abstract** The aim of the present study was to assess, by Raman spectroscopy and laser fluorescence, the repair of surgical fractures fixed with wire osteosynthesis treated or not with infrared laser (λ780 nm, 50 mW, 4×4 J/cm$^2$=16 J/cm$^2$, $\phi$=0.5 cm$^2$, CW) associated or not to the use of hydroxyapatite and guided bone regeneration. Surgical tibial fractures were created under general anesthesia on 15 rabbits that were divided into five groups, maintained on individual cages, at day/night cycle, fed with solid laboratory pelted diet, and had water ad libitum. The fractures in groups II, III, IV, and V were fixed with wires. Animals in groups III and V were grafted with hydroxyapatite (HA) and guided bone regeneration (GBR) technique used. Animals in groups IV and V were irradiated at every other day during 2 weeks (4×4 J/cm$^2$, 16 J/cm$^2$=112 J/cm$^2$). Observation time was that of 30 days. After animal death, specimens were taken and kept in liquid nitrogen and used for Raman spectroscopy. The Raman results showed basal readings of 1,234.38±220. Groups WO+B+L showed higher readings (1,680.22±822) and group WO+B the lowest (501.425±328). Fluorescence data showed basal readings of 5.83333±0.7. Groups WO showed higher readings (6.91667±0.9) and group WO+B+L the lowest (1.66667±0.5). There were significant differences between groups on both cases ($p$<0.05). Pearson correlation was negative and significant ($R^2$=−0.60; $p$< 0.001), and it was indicative that, when the Raman peaks

A. L. B. Pinheiro (✉) · N. R. S. Santos · P. C. Oliveira · G. T. S. Aciole · T. A. Ramos · T. A. Gonzalez · L. N. da Silva · A. F. S. Barbosa
Center of Biophotonics, School of Dentistry,
Federal University of Bahia,
Av. Araújo Pinho, 62, Canela,
Salvador, BA 40110-150, Brazil
e-mail: albp@ufba.br

N. R. S. Santos
e-mail: ribeironicole@hotmail.com

P. C. Oliveira
e-mail: pchagas2005@yahoo.com.br

G. T. S. Aciole
e-mail: gilberthaciole@hotmail.com

T. A. Ramos
e-mail: thais_andraderamos@hotmail.com

T. A. Gonzalez
e-mail: tayna_gonzalez@yahoo.com.br

L. N. da Silva
e-mail: lay_lica@hotmail.com

A. F. S. Barbosa
e-mail: arturfelipes@gmail.com

A. L. B. Pinheiro · L. Silveira Jr
Universidade Camilo Castelo Branco Núcleo do Parque Tecnológico de São José dos Campos,
Rodovia Presidente Dutra, km. 138 - Distrito de Eugenio de Melo,
São José dos Campos, 12247-004, SP, Brazil

L. Silveira Jr
e-mail: land-jr@uol.com.br

A. L. B. Pinheiro
Instituto Nacional de Ciência e Tecnologia de Óptica e Fotônica,
São Carlos, SP, Brazil 13560-970

of calcium hydroxyapatite (CHA) are increased, the level of fluorescence is reduced. It is concluded that the use of near-infrared lasertherapy associated to HA graft and GBR was effective in improving bone healing on fractured bones as a result of the increasing deposition of CHA measured by Raman spectroscopy and decrease of the organic components as shown by the fluorescence readings.

**Keywords** Biomaterials · Bone repair · Internal rigid fixation · Phototherapy

## Introduction

The discovery of anesthesia allowed a significant advance on the treatment of fractures, such as the use of direct intra-osseous wires. The treatment of fractures consists of the reduction and fixation of dislocated segments [1]. Internal fracture fixation provides mechanical stability to a fractured bone, allowing weight bearing, early use of the affected bone, and rapid bone healing. It is indicated when anatomical reduction is essential, as with articular or growth plate fractures. The selection of internal fixation is based on multiple mechanical, biologic, and clinical parameters associated with each patient and fracture, not just the fracture pattern itself [2]. The choice of internal fixation depends on the type of fracture, the condition of the soft tissues and bone, the size and position of the bone fragments, and the size of the bony defect. Numerous devices are available for internal fixation. These devices can be roughly divided into a few major categories: wires; pins and screws; plates; and intramedullary nails or rods. Staples and clamps are also used occasionally for osteotomy or fracture fixation [3, 4].

Stainless steel wire is the traditional material used for fracture fixation because it is a biologically inert material; rigid; provides precise repositioning of the bone fragments; easy to use; and has a reasonable cost [5]. Although internal fixation provides superb mechanical support, it is usually disruptive to the biologic environment. Internal fixation requires a surgical approach; thus, it disrupts the soft tissues and vascularity surrounding the fracture. Attempts are always made to provide the most rigid mechanical fixation while minimizing the surgical trauma [6]. Inter-fragmentary micro-motion causes high levels of strain on the fracture ends, leading to bone resorption, followed by callus formation and transformation of fibrocartilage to bone. This is common when pins and wires are the only fixations utilized [7].

Despite that small rodents possess only a primitive bone structure without a Haversian system, their fracture repair processes are similar to larger mammalians [8]. Therefore, this model may be used to investigate bone repair [9]. Several murine models using long bone fractures are commonly described analyzing therapeutic options of different stabilization techniques or the systemic influence of an additional impact in trauma models. Due to the small size, only large long bones, especially tibia and femur, have been studied [10]. Similar to murine models, rats are used investigating fracture healing. However, due to the missing Haversian system, intra-cortical remodeling cannot be detected in rats representing an essential difference to humans [11]. Similar to murine models, the fracture may be technically simulated by an osteotomy or fractured manually after weakening the bone [12, 13]. To stabilize the fracture, an intramedullary pin or wire may be used [14].

There are fractures in which handling is further complicated due to the loss of bone. These losses may be related to several etiologies and require further efforts from the body to fully recover. Although grafts have been used to minimize the problems associated to bone losses, considerable limitations associated with autografts and allografts have prompted increased interest in alternative bone graft substitutes. The main types of commercially available bone graft substitutes are demineralized allograft bone matrix; ceramics and ceramic composites; composite graft of collagen and mineral; coralline hydroxyapatite; calcium phosphate cement; bioactive glass; and calcium sulfate [15–17].

The healing of various types of bone defect with complete bone fill has been reported following the use of the guided bone regeneration (GBR) technique [18]. GBR is a technique used to prevent the migration of soft tissues, which has more pronounced proliferative activity, into the bone defect. GBR promotes bone formation by the use of a mechanical barrier such as membranes, and these may be reabsorbable or non-reabsorbable and may also be associated or not to bone substitutes. The GBR is widely used for treating periodontal defects and other bone defects [19].

Raman scattering is a powerful light scattering technique used to diagnose the internal structure of molecules and crystals. Raman spectroscopy is the measurement of the wavelength and intensity of inelastically scattered light from molecules. The Raman scattered light occurs at wavelengths that are shifted from the incident light by the energies of molecular vibrations. The mechanism of Raman scattering is different from that of infrared absorption, and Raman and infrared (IR) spectra provide complementary information. Typical applications are in structure determination, multi-component qualitative analysis, and quantitative analysis [3, 4]. Its use allows less invasive and nondestructive analysis of biological samples, allowing one to get precise information on biochemical composition. It has been considered effective to assess tissues at the molecular level and has been used on several noninvasive diagnostic applications of biological samples such as cancer; human coronary arteries; blood analysis; implants; cell culture; bone disease; and bone healing and to evaluate the microstructure of human cortical bone (osteon) and biomaterials.

We have used Raman spectroscopy as a method of assessment of the effects of laser phototherapy (LPT) on bone healing under different models [20–24], including fractures [3, 4]. Our previous results indicate that near-infrared (NIR) LPT is effective to improve bone repair mainly due to its higher penetration into bone when compared with visible laser light [15–17, 19, 25, 26]. The use of LPT on studies involving bone healing is a hot topic lately, and many have demonstrated positive stimulatory effects even when associated to biomaterials [3, 4, 15, 17, 19–24, 26–29].

By using infrared excitation (λ785 or λ830 nm), one can minimize the interference of the autofluorescence on the Raman spectra from biological specimens [3, 4]. On the other hand, there are molecules capable of interacting with light in a different way. The absorption of the light occurs on the chromophores that are molecules capable of absorbing and emitting light by fluorescence. The absorbing sites are known as fluorophores. These molecules will absorb energy of a specific wavelength and re-emit energy at a different (but equally specific) wavelength. The amount and wavelength of the emitted energy will depend on both the fluorophore and on its chemical environment. On this group, we may include flavins, proteins, collagen, elastin, NADH, and porphyrins. This is the case of a commercial device called DIAGNOdent®.

Many molecules are able to interact with light by its absorption by chromophores that, on molecules also capable of emitting light (fluorescence), are known as fluorophores. These structures will absorb energy of a specific wavelength and re-emit it at a different, but equally specific, wavelength. Flavins, proteins, collagen, elastin, NADH, and porphyrins are fluorophores. The intensity of the fluorescence is directly related to the amount of fluorophores at the site. Fluorescence on living organisms is mainly related to organic components; apatite also plays a small role in that [30–32].

The DIAGNOdent® (λ655 nm, modulated, 1 mW peak power diode laser combined with a long pass filter transmission >λ680 nm as the detector) was used initially for the diagnosis of dental caries, but we have used it previously as an optical biopsy method to assess bone healing on tibial fractures [29]. We found that Pearson correlation showed that fluorescence readings correlated negatively with the Raman data and concluded that the use of both methods indicates that the use of the biomaterials associated with infrared LPT resulted in a more advanced and higher quality of bone repair in fractures treated with miniplates and that the device may be used to perform optical biopsy on bone [29].

In summary, fractures are common and disabling lesions. It may be treated by means of several techniques and devices. The choice of the treatment depends on the type, site, and etiology of the trauma. Usually, internal fixation of the fragments either by platting or wiring is the method of choice as they reduce dislocation of the fragments preventing fibrosis and reducing the gap between fragments. Platting is most often the recommended choice; however, it is costly. Wire osteosynthesis is the second option as it is semi-rigid. In cases of large bone losses, the use of bone grafts and membrane is recommended. The use of light to improve bone repair has been widely reported in the literature. These aspects prompted us to study if improvement of the repair of fractures treated by wiring, biomaterial, membrane, and laser would result in a repair similar to the one observed when platting is used, as a way of possibly reducing the cost of the treatment.

The aim of this study was to evaluate, by laser fluorescence and Raman spectroscopy, the repair of complete tibial fracture in rabbits treated by wire osteosynthesis associated or not to the use of a biphasic ceramic graft associated or not to the use of GBR and irradiated or not with λ780 nm laser in rabbits.

## Materials and methods

The Animal Ethics Committee of the School of Dentistry of the Federal University of Bahia has approved this research. Fifteen healthy adult male New Zealand rabbits (~8 months old; mean weight, 2 kg) were kept under natural conditions of light, humidity, and temperature at the Laboratory of Animal Experimentation of the School of Dentistry of the Federal University of Bahia during the experimental period. The animals were fed with standard laboratory pelted diet and had water ad libitum. The animals were kept in individual metallic gages; kept at day/night light cycle; and controlled temperature during the experimental period. The animals were randomly distributed into five groups (Table 1).

Prior intramuscular general anesthesia, the animals received acepromazine (2 mg/kg Acepran®, 0.2 % Univet S.A, Cambuci, SP, Brazil). The anesthesia was carried out 20 min later with ketamine (Ketalar®, 50 mg/ml 0.4 ml/kg, Lab. Parke Davis Ltd, São Paulo, SP, Brazil) and 2 % xylazine (Rompum®, 20 mg/ml 0.2 ml/kg, Lab. Bayer Health Care S.A., São Paulo, SP, Brazil). The animals had the right leg shaved, and a 3-cm-long incision was performed at the right tibia with a no. 15 scalpel blade. Skin and subcutaneous tissues were dissected down to the periosteum, which was gently sectioned, exposing the bone. A complete surgical tibial fracture was created on animals in groups II, III, IV, and V with a carborundum disk (Moyco Union Broach, York, PA, USA) under water refrigeration.

Animals in group II had the bone fragments fixed with wire osteosynthesis (0.3 mm, Morelli®, Sorocaba, SP, Brazil). Animals in groups III and V were grafted with the 0.5-

**Table 1** Description and distribution of the groups on the study

| Group | Procedure | Description |
|---|---|---|
| I | Basal bone | Control–no fracture |
| II | Wire osteosynthesis (WO) | Fracture fixed with wire only |
| III | Wire osteosynthesis+biomaterial (WO+B) | Fracture fixed with wire+Genphos®+Genderm® |
| IV | Wire osteosynthesis+laser (WO+L) | Fracture fixed with wire+laser |
| V | Wire osteosynthesis+biomaterial+laser (WO+B+L) | Fracture fixed with wire+Genphos®+Genderm®+laser |

mm particle ceramic graft (GenPhos® HATCP. BAUMER®, Mogi Mirim, SP, Brazil) and covered with a demineralized bovine bone membrane (Gen-derm®, BAUMER®, Mogi Mirim, SP, Brazil) prior similar fixation used on group I (Fig. 1). Animals in groups IV and V were further irradiated with laser light (λ780 nm, 50 mW, CW, spot area of 0.5 $cm^2$,[1] TWIN FLEX®, MM Optics, São Carlos, SP, Brazil). The irradiation started immediately after treatment prior suturing (16 $J/cm^2$, 4×4 $J/cm^2$, 9 J per point) and was transcutaneously repeated at every other day during 2 weeks. After suturing (4-0 polyglactin, TRUSINTH®, Sutures India Pvt Ltd. Bangalore, Karnataka, India) and (4-0 nylon, TRUSINTH®, Sutures India Pvt Ltd. Bangalore, Karnataka, India), the animals received intramuscular antibiotics (Pentabiótico®, penicillin, streptomycin, 20.000 UI 0.2 ml/Kg IM, Lab. Forte Dogde Saúde Animal Ltda, Campinas, SP, Brazil) and (Banamine®, flunixinmeglumine, 10 mg/ml, 0.1 ml/kg IM, Intervet Schering-Plough Animal Health, Cruzeiro, SP, Brazil).

## Fluorescence readings

A commercial device (DIAGNOdent 2095®) was used to collect the fluorescence readings (λ665 nm) according to the instructions of the manufacturer (Kavo, Germany). Prior to the analysis of the specimens, a pilot study determined the mean values of the readings at the surface (baseline) of non-treated subjects. The data were statistically analyzed, and no significant differences were found between the readings of the tested samples ($p>0.001$). On the experimental specimens, the data were collected twice: prior to the experiment (baseline, four points at the surface) and at the end of the experimental time before the removal of the specimen (four points at the fracture surface). The results were analyzed using Minitab 15.0® software (Minitab, Belo Horizonte, MG, Brazil). Data normality was assessed by the Kolmogorov–Smirnov test. ANOVA and Student's *t* tests were used to identify differences between groups.

[1] Beam area was measured with a calibrated digital caliper.

## Raman spectroscopy

Following animal death 30 days after fracture, the samples were longitudinally cut under refrigeration (Bueler®, Isomet TM1000; Markham, Ontario, Canada) and stored in liquid nitrogen to minimize the growth of aerobic bacteria and because the chemical fixation is not advisable due to fluorescence emissions from the fixative substances [3, 4, 29, 33].

Prior to Raman study, the samples were longitudinally cut and warmed gradually to room temperature, and 100 mL of saline was added to the surface during spectroscopic measurements. For Raman measurements, a Raman system (P-1, Lambda Solutions, Inc., MA, USA) was used. Acquisition and storage of the Raman data were done with a PC (Dell Inspiron mod. 1501) and RamaSoft® software (Lambda Solutions, Inc., MA, USA). The laser power used at the sample site was of 100 mW with spectral acquisition time 10 s. Three points were measured at the fractured site of each specimen. All spectra were collected on the same day to avoid optical misalignments and changes in laser power. The mean value of the intensity of the peak (~958 $cm^{-1}$, phosphate $\nu_1$) was determined by the average of the peaks on this region. This intensity is related to the concentration of calcium hydroxyapatite (CHA) of the bone. For calibration, the Raman spectrum of the solvent indene with known peaks was used due to its intense bands (800–1,800 $cm^{-1}$) in the fingerprint region [3, 4, 29, 33].

The indene spectrum was also measured each time the sample was changed to be sure that the laser and collection optics were optimized. In order to remove the "fluorescence background" from the original spectrum, a fifth-order polynomial fitting was found to give better results facilitating the

**Fig. 1** Final setup of the surgical site. Note the presence of the wire and membrane covering the particles of the biomaterial

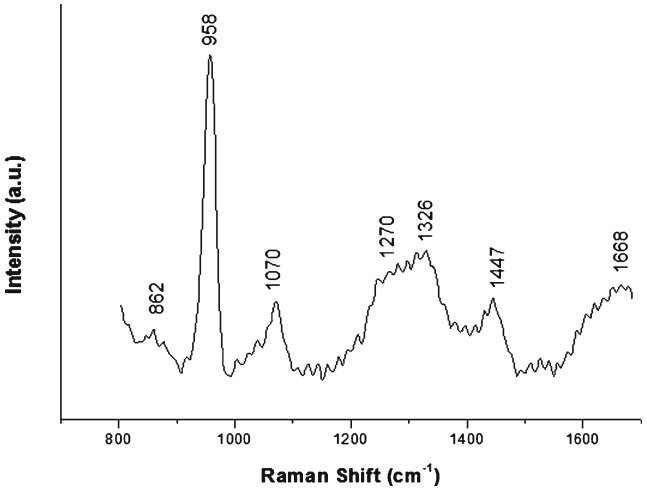


**Fig. 2** Diagram showing the main Raman peaks observed on bone tissue

visualization of the peaks of CHA (~958 $cm^{-1}$) found on the bone. A baseline Raman spectrum of non-treated bone (group I) was also produced and acted as control (Fig. 2). The data were analyzed by the MatLab5.1® software (Newark, NJ, USA) for calibration and background subtraction of the spectra. Statistical analysis was performed using Minitab 15.0® software (Minitab, Belo Horizonte, MG, Brazil). Correlation between Raman and fluorescence data was carried out with Pearson correlation. Significance level in all cases was set at 5 %.

## Results

The Raman spectrum of bone shows prominent vibrational bands related to tissue composition (mineral and organic matrices). Figure 2 shows the bone main Raman bands at 862, 958, 1,070, 1,270 and 1,326, 1,447, and 1,668 $cm^{-1}$. The band at 1,668 $cm^{-1}$ and the ones at 1,270 and 1,326 $cm^{-1}$ are attributed to amide I and III stretching modes of lipids and proteins; the band at 1,447 $cm^{-1}$ is attributed to the bending and stretching vibration modes of CH groups of lipids and proteins. The ones at 958 and 1,070 $cm^{-1}$ are attributed to phosphate and carbonate hydroxyapatite (HA) from bone mineral, respectively; the band at 862 $cm^{-1}$ may be attributed to the vibration bands of C–C stretch of collagen (tyrosine/proline ring).

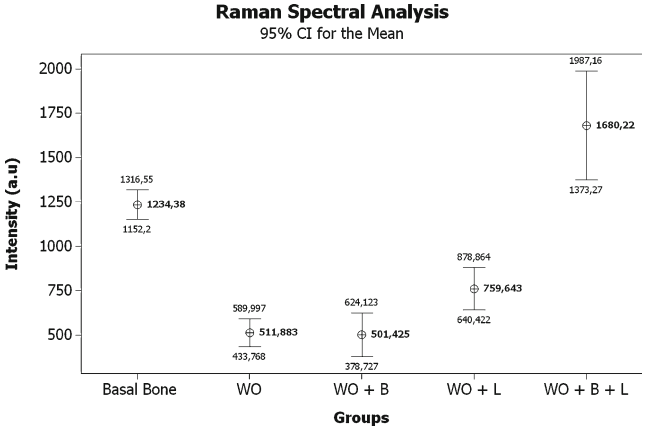


**Fig. 4** Mean intensity of the peak of CHA (~958 $cm^{-1}$) on control and treated animals

Figure 3 shows the mean spectra (dislocated) of CHA (~958 $cm^{-1}$) on control and treated animals. The intensity of the Raman shift is directly related to the concentration/incorporation of CHA by the bone. So, higher intensity represents higher concentration of CHA. Basal readings showed a mean value of 1,234.38±220. Groups WO+B+L showed higher readings (1,680.22±822) and group WO+B the lowest (501.425±328) (Fig. 4). Table 2 shows a summary of the statistical analysis.

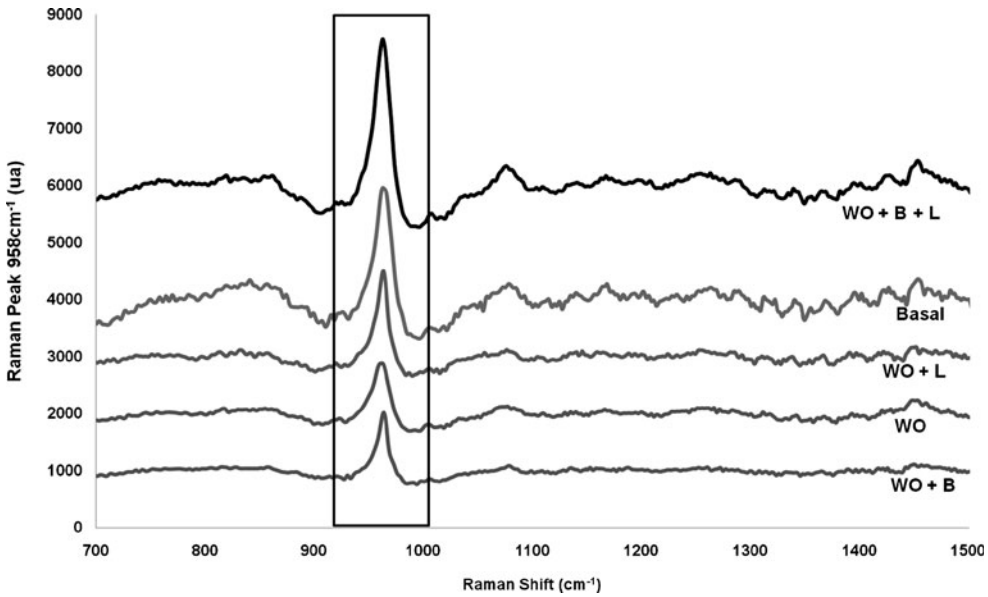


**Fig. 3** Spectra of basal and experimental groups. Each individual spectrum is dislocated to reflect the mean value of the peak of CHA (~958 $cm^{-1}$)

**Table 2** Mean and standard deviation of the peaks of the Raman shift of CHA (~958 $cm^{-1}$) on the groups

| Group | Média±DP |
|---|---|
| Basal Bone a | 1,234.38±220 b,c,d,e |
| WO b | 511.883±209 a,d |
| WO+B c | 501.425±328 a,d,e |
| WO+L d | 759.643±319 a,b,c,e |
| WO+B+L e | 1,680.22±822 a,b,c,d |

Letters on right-hand side column indicate the occurrence of significant differences between groups on the left-hand side column

$p \leq 0.05$

**Table 3** Mean and standard deviation of the fluorescence (a.u) readings on the groups

| Group | Mean±SD |
|---|---|
| Basal bone a | 5.8333±0.7 b,c,d,e |
| WO b | 6.91667±0.9 a,c,e |
| WO+B c | 3±1.4 a,b,d,e |
| WO+L d | 6.58333±0.9 a,c,e |
| WO+B+L e | 1.66667±0.5 a,c,d |

Letters on right-hand side column indicate the occurrence of significant differences between groups on the left-hand side column

$p \leq 0.05$

Fluorescence basal readings showed a mean value of 5.83333±0.7; group WO showed higher readings (6.91667 ±0.9) and group WO+B+L the lowest (1.66667±0.5) (Fig. 5). A summary of the fluorescence readings and statistical analysis may be seen on Table 3.

Pearson correlation was negative and significant ($R^2 = -0.60$; $p < 0.001$), and it was indicative that, when the Raman peaks of CHA are increased, the level of fluorescence is reduced (Fig. 6).

## Discussion

Raman spectroscopy may be used to access the molecular constitution of a specific tissue and then classify it according to differences observed in the spectra [34, 35]. Several studies found elsewhere on the literature has shown successful use of near-infrared spectroscopy (NIRS) as a diagnostic tool for healthy, diseased, or healing bones [3, 4, 27, 29, 33–35]. We have successfully used Raman spectroscopy to determine both mineral and organic component changes on the healing bone. This method of assessment is considered by our team and others as a gold standard to study bone components [3, 4, 27, 29, 33–35].

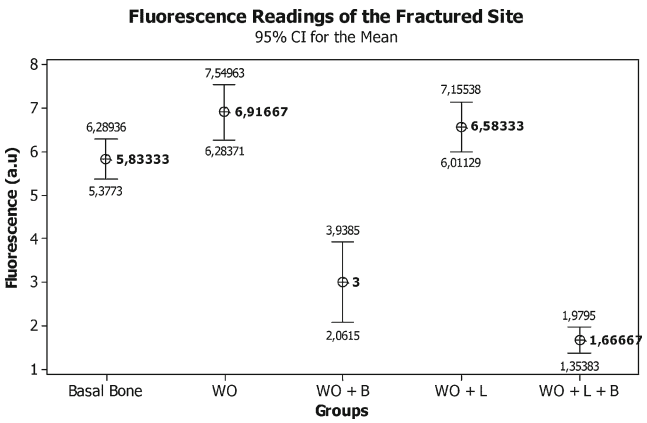


**Fig. 5** Mean fluorescence readings on control and treated animals

The DIAGNOdent® is a device originally designed to diagnose caries. The literature reported the detection of tricalciumphosphate, dicalciumphosphate-dihydrate, and calcium carbonate measured by fluorescence of pure pellets with excitation at λ655 nm. It is important to mention that it has been shown that this device presents good reproducibility both in vivo and in vitro. We found only one report on the literature on the use of this device as an optical biopsy method, and similar to that report, we decided to use Raman spectroscopy as gold standard [29].

One of the models we have used for assessing the effects of laser light on bone is the complete tibial fracture one. This model is very complex and allows several treatment approaches. These include the use WO and miniplates. Associated to these treatment methods, we have also associated them to biomaterials and guided bone regeneration [3, 4, 29].

The use of phototherapies has been successfully reported for the improvement of bone repair under different conditions [3, 4, 15, 20–24, 29, 30, 33]. The effects of the use of light sources on bone are still controversial, as previous reports show different or conflicting results. It is possible

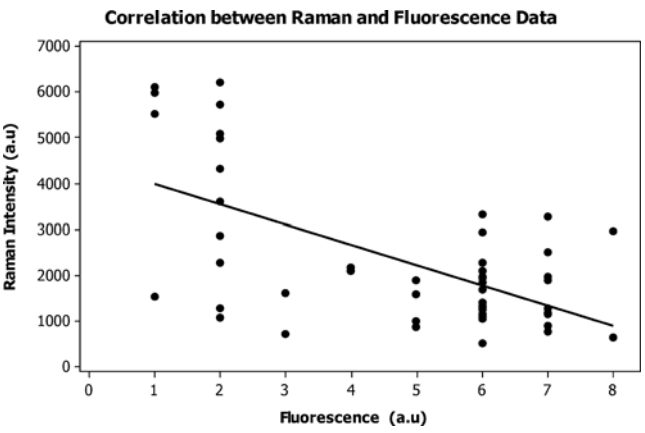


**Fig. 6** Graphical illustration of the Pearson correlation. It is shown as a negative and significant correlation being indicative that, when the Raman peaks of CHA are increased, the level of fluorescence was reduced

that the effect of different light sources on bone regeneration depends not only on the total dose of irradiation but also on the irradiation time and the irradiation mode [3, 4, 15, 20–24, 29, 30, 33].

Many studies indicated that irradiated bone, mostly with IR wavelengths, shows increased osteoblastic proliferation, collagen deposition, and bone neo-formation when compared with non-irradiated bone [3, 4, 15, 20–24, 29, 30, 33]. The irradiation protocol used in this study is similar to those used on previous reports [3, 4, 15, 20–24, 29, 30, 33]. Our group has shown, using different models, that association of bone grafts, BMPs, and guided tissue regeneration does improve the healing of bone tissue [3, 4, 15, 20–24, 29, 30, 33].

In all protocols, models, and parameters we used previously, we were able to demonstrate that NIR LPT caused important tissue responses during healing, and these were responsible for a quicker repair process as well as on the improved quality of the newly formed bone [3, 4, 15, 20–24, 29, 30, 33].

We only found a previous report using a similar model to the one used in the present study, and the complete understanding of our results remains difficult [3]. There are several aspects to consider with regard to the technique used. Initially, it is important to consider that the repair of fractured bones is lengthy, when compared with other types of bony defects, and demands stability of the fragments in order not to develop nonunion. In our study, no such case was found. The present investigation was analyzed by NIRS, the intensity of the shift of the CHA (~958 $cm^{-1}$) [3], and fluorescence [29] of sites of complete tibial fractures in rabbits. The fractures were routinely treated by open reduction and internal fixation using wire osteosynthesis [3].

The irradiation protocol used on the present study was based upon previous reports [3, 4, 15, 20–24, 29, 30, 33]. We have previously found that the levels of CHA on deep areas of healing bone of irradiated and non-irradiated subjects differ significantly from day 30 after treatment [3, 4, 15, 20–24, 29, 30, 33]. In this study, we were able to detect differences on the CHA levels of fractured sites when internal fixation was associated to the use of biomaterial and lasertherapy. On the present study, the intensity of the Raman shift was found being directly related to the concentration/incorporation of CHA by the bone. So, higher intensity represented higher concentration of CHA. The Raman results showed basal readings of 1,234.38±220, and group WO+B+L was the one with higher readings (1,680.22± 822), and group WO+B showed the lowest (501.425±328). The fluorescence data are coherent with the Raman data as these showed basal readings of 5.83333±0.7, and groups WO presented higher readings (6.91667±0.9) and group WO+B+L the lowest (1.66667±0.5). It is important to notice that the Pearson correlation was negative and significant ($R^2$=−0.60; $p$<0.001), and it was indicative that, when the Raman peaks of CHA were increased, the level of fluorescence was reduced (Fig. 6). This was expected, as the Raman data were associated to the levels of mineralization and the fluorescence data to the level of demineralization. This is in complete agreement with our previous report [29]. The use of both methods indicates that the use of the biomaterial associated to NIR LPT resulted on a more advanced quality bone repair on fractures treated with WO and that the DIAGNOdent® may be used to perform optical biopsy on bone.

It is concluded that the use of NIR laser phototherapy associated to HA graft and GBR was effective in improving bone healing on fractured bones as a result of the increasing deposition of CHA measured by Raman spectroscopy and decrease of the organic components as shown by the fluorescence readings.

## References


1. Erdogan O, Esen E, Ustun Y, Kurkçu M, Akova T, Gonlusen G, Uysal H, Çevlik F (2006) Effects of low-intensity pulsed ultrasound on healing of mandibular fractures: an experimental study in rabbits. J Oral Maxillofac Surg 64:180–188
2. Aron DN, Palmer RH, Johnson AL (1995) Biologic strategies and a balanced concept for repair of highly comminuted long bone fractures. Compend Contin Educ Pract Vet 17:35–49
3. Lopes CB, Pacheco MTT, Silveira Junior L, Duarte J, Cangussu MCT, Pinheiro ALB (2007) The effect of the association of NIR laser therapy BMPs, and guided bone regeneration on tibial fractures treated with wire osteosynthesis: Raman spectroscopy study. J Photochem Photobiol B Biol 89:125–130
4. Lopes CB, Pacheco MTT, Silveira-Junior L, Cangussu MC, Pinheiro ALB (2010) The effect of the association of near infrared laser therapy, bone morphogenetic proteins, and guided bone regeneration on tibial fractures treated with internal rigid fixation: a Raman spectroscopic study. J Biomed Mater Res A 94:1257–1263
5. Broaddus WC, Holloway KL, Winters CJ, Bullock MR, Graham RS, Mathern BE, Ward JD, Young HF (2002) Titanium miniplates or stainless steel wire for cranial fixation: a prospective randomized comparison. J Neurosurg 96:244–247
6. Hulse D, Hyman B (2003) Fracture biology and biomechanics. In: Slatter D (ed) Textbook of small animal surgery, 3rd edn. Saunders, Philadelphia, pp 1785–1792
7. Stiffler KS (2004) Internal fracture fixation. Clin Tech Small Anim Pract 19:105–113
8. Nunamaker DM (1998) Experimental models of fracture repair. Clin Orthop Relat Res 355:S56–S65
9. Holstein JH, Garcia P, Histing T et al (2009) Advances in the establishment of defined mouse models for the study of fracture healing and bone regeneration. J Orthop Trauma 23:S31–S38
10. Marturano JE, Cleveland BC, Byrne MA, O'Connell SL, Wixted JJ, Billiar KL (2008) An improved murine femur fracture device for bone healing studies. J Biomech 41:1222–1228
11. Manabe T, Mori S, Mashiba T et al (2007) Human parathyroid hormone (1–34) accelerates natural fracture healing process in the femoral osteotomy model of cynomolgus monkeys. Bone 40:1475–1482
12. Utvag SE, Korsnes L, Rindal DB, Reikerås O (2001) Influence of flexible nailing in the later phase of fracture healing: strength and mineralization in rat femora. J Orthop Sci 6:576–584

13. Schoen M, Rotter R, Schattner S et al (2008) Introduction of a new interlocked intramedullary nailing device for stabilization of critically sized femoral defects in the rat: a combined biomechanical and animal experimental study. J Orthop Res 26(1):84–189
14. Frink M, Andruszkow H, Zeckey C, Krettek C, Hildebrand F (2011) Experimental trauma models: an update. J Biomed Biotechnol. doi:10.1155/2011/797383
15. Pinheiro ALB, Gerbi MEMM (2006) Photoengineering of bone repair processes. Photomed Laser Surg 24:169–178
16. Weber JB, Pinheiro ALB, Oliveira MG, Oliveira MGO, Ramalho LMP (2006) Laser therapy improves healing of bone defects submitted to autologous bone graft. Photomed Laser Surg 24:38–44
17. Pinheiro ALB, Limeira Junior FA, Gerbi MEMM, Ramalho LMP, Marzola C, Ponzi EAC (2003) Effect of low level laser therapy on the repair of bone defects grafted with inorganic bovine bone. Braz Dent J 14:177–181
18. Donos N, Kostopoulos L, Karring T (2002) Augmentation of the mandible with GTR and onlay cortical bone grafting. An experimental study in the rat. Clin Oral Implants Res 13:175–184
19. Gerbi MEMM, Pinheiro ALB, Marzola C, Limeira Junior F, Ramalho LMP, Ponzi EAC, Soares AO, Carvalho LCB, Lima HCAV, Gonçalves TO (2005) Assessment of bone repair associated with the use of organic bovine bone and membrane irradiated at 830-nm. Photomed Laser Surg 23:382–388
20. Pinheiro ALB, Gerbi MEMM, Limeira Junior FA et al (2009) Bone repair following bone grafting hydroxyapatite guided bone regeneration and infra-red laser photobiomodulation: a histological study in a rodent model. Lasers Med Sci 24:234–240
21. Gerbi MEMM, Marques AMC, Ramalho LMP et al (2008) Infrared Laser light further improves bone healing when associated with bone morphogenic proteins: an in vivo study in a rodent model. Photomed Laser Surg 26:55–60
22. Pinheiro ALB, Gerbi MEMM, Ponzi EAC et al (2008) Infrared laser light further improves bone healing when associated with bone morphogenetic proteins and guided bone regeneration: an in vivo study in a rodent model. Photomed Laser Surg 26:167–174
23. Torres CS, Santos JN, Monteiro JSC, Gomes PTCC, Pinheiro ALB (2008) Does the use of laser photobiomodulation, bone morphogenetic proteins, and guided bone regeneration improve the outcome of autologous bone grafts? An in vivo study in a rodent model. Photomed Laser Surg 26:371–377
24. Gerbi MEMM, Pinheiro ALB, Ramalho LMP (2008) Effect of IR laser photobiomodulation on the repair of bone defects grafted with organic bovine bone. Lasers Med Sci 23:313–317
25. Pinheiro ALB, Limeira Júnior FA, Gerbi MEMM et al (2003) Effect of 830-nm laser light on the repair of bone defects grafted with inorganic bovine bone and decalcified cortical osseous membrane. J Clin Laser Med Surg 21:383–388
26. Pinheiro ALB, Oliveira MAM, Martins PPM (2001) Biomodulação da cicatrização óssea pós-implantar com o uso da laserterapia não-cirúrgica: estudo por microscopia eletrônica de varredura. Rev FOUFBA 22:12–19
27. Lopes CB, Pinheiro ALB, Sathaiah S, Duarte J, Martins MC (2005) Infrared laser light reduces loading time of dental implants: a Raman spectroscopy study. Photomed Laser Surg 23:27–31
28. Silva Junior AN, Pinheiro ALB, Oliveira MG, Weissmann R, Ramalho LMP, Nicolau RA (2002) Computadorized morphometric assessment of the effect of low-level laser therapy on bone repair: an experimental animal study. J Clin Laser Med Surg 20:83–88
29. Pinheiro ALB, Lopes CB, Pacheco MTT, Brugnera A, Zanin FAA, Cangussú MCT, Silveira-Junior L (2010) Raman spectroscopy validation of DIAGNOdent-assisted fluorescence readings on tibial fractures treated with laser phototherapy, BMPs, guided bone regeneration, and miniplates. Photomed Laser Surg 28:89–97
30. Pinheiro ALB, Aciole GTS, Cangussú MCT, Pacheco MTT, Silveira-Junior L (2010) Effects of laser phototherapy on bone defects grafted with mineral trioxide aggregate, bone morphogenetic proteins, and guided bone regeneration: a Raman spectroscopic study. J Biomed Mater Res A 95:1041–1047
31. Shi Q, Tranaeus S, Angmar-Mansson B (2001) Validation of DIAGNOdent for quantification of smooth-surface caries: an in vitro study. Acta Odontol Scand 59:74–78
32. Hibst R, Paulus R, Lussi A (2001) Detection of occlusal caries by laser fluorescence. Basic and clinical investigations. Med Laser Appl 16:205–213
33. Lopes CB, Pinheiro ALB, Sathaiah S, Silva NS, Salgado MC (2007) Infrared laser photobiomodulation (830 nm) on bone tissue around dental implants: a Raman spectroscopy and scanning electron microscopy study in rabbits. Photomed Laser Surg 25:96–101
34. Penel G, Delfosse C, Descamps M, Leroy G (2005) Composition of bone and apatitic biomaterials as revealed by intravital Raman microspectroscopy. Bone 36:893–901
35. Carden A, Morris MD (2000) Application of vibrational spectroscopy to the study of mineralized tissues (review). J Biomed Opt 5:259–268